7.6 Optimal Jet Selection Logic

In this section, a brief introduction to the Space Shuttle on-orbit reaction control system is followed by a description of the optimal jet selection problem of advanced space vehicles with strongly three-axis coupled, redundant sets of thrusters for both translation and rotation control.

7.6.1 Space Shuttle On-Orbit Reaction Control System

The Space Shuttle has two orbital maneuvering system (OMS) engines, each producing about 26,700 N (6000 lb) of thrust. They are bipropellant rockets with a specific impulse of 313 s, and used mainly for large orbit-change ΔV maneuvers. Each OMS engine has redundant two-axis gimbal capability.

The Space Shuttle on-orbit reaction control system (RCS) consists of 38 primary jets, each producing about 3870 N (870 lb) of thrust, and 6 vernier jets, each producing about 107 N (24 lb) of thrust. All thrusters using the same bipropellant as the OMS have 80-ms minimum pulse granularity. The thrusters are located in three pods: forward, left aft, and right aft. The primary jets are divided into 14 clusters around the vehicle with both translational and rotational control capabilities and with multiple failure tolerance. The vernier jets, however, each fire in a different direction, only control rotation, and have no failure tolerance if any one of four of the thrusters malfunctions. Figure 7.8 illustrates thruster locations and plume directions with an explanation of the thruster identification nomenclature [53–55].

The Space Shuttle RCS processor with a 12.5-Hz sampling rate consists of phase-plane and jet selection logic. The phase-plane logic in general performs on–off modulation of jet torque commands as required to maintain vehicle attitude and rate errors within the specified deadbands. In addition, desired angular rate change is also computed to facilitate computation of jet burn times. The phase plane of angular rate vs attitude angle, per each axis, consists of a set of switch lines for specified attitude deadbands, angular rate limits, and expected RCS accelerations. As illustrated in Fig. 7.9, the phase plane is divided into nine regions defined by numbered boundaries. At any time, for each axis, the rigid vehicle state is defined by an attitude and rate error point that must lie in one of the defined regions because the regions cover the entire plane. The decision concerning whether to send a rotation command is made on the basis of logic unique to each region. Regions 1 and 5 always command jets. For primary jets, regions 2, 3, 6, and 7 always permit coast with no jet commands. Region 9 never causes commands to be generated, but a preference for vernier jet selection is computed. Regions 4 and 8 have hysteresis. If the phase point is in either region 4 or 8 and a jet firing is taking place, then the firing will continue until the phase point crosses the S13 switch curve [53].

The jet selection logic identifies specific jets to be used. For primary jets it uses a table lookup scheme with selection details dependent on flight phase, selected modes, and recognized jet failure status. For vernier jets it utilizes a dot-product algorithm. The principle of the dot-product algorithm is to take the dot product of each jet's rotational velocity increment vector with a vector from the rotation

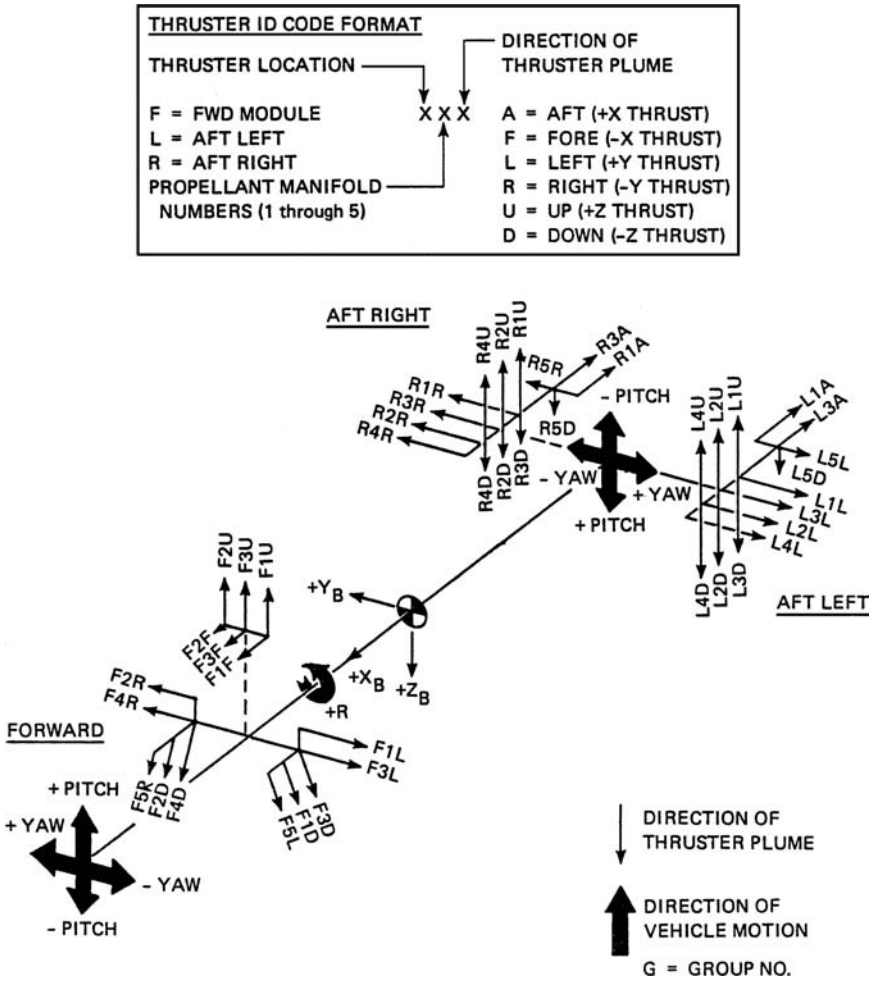

Fig. 7.8 Space Shuttle thruster locations and plume directions.

commands and then select the jets with the biggest dot-product values. The baseline RCS processor excludes mixed operations of primary and vernier jets.

During the early Shuttle program, a new autopilot concept was developed by Bergmann et al. [56] at the Charles Stark Draper Laboratory, which promised certain advantages over the conventional phase-plane logic based on a table lookup scheme for jet selection. The new autopilot concept incorporated a six-dimensional "phase space" control logic and a linear programming algorithm for jet selection. The unique features of this new autopilot scheme include: fuel-optimal jet selection, a high degree of adaptability to configuration changes and jet failures, combined primary and vernier jet usage, and closed-loop translation control.

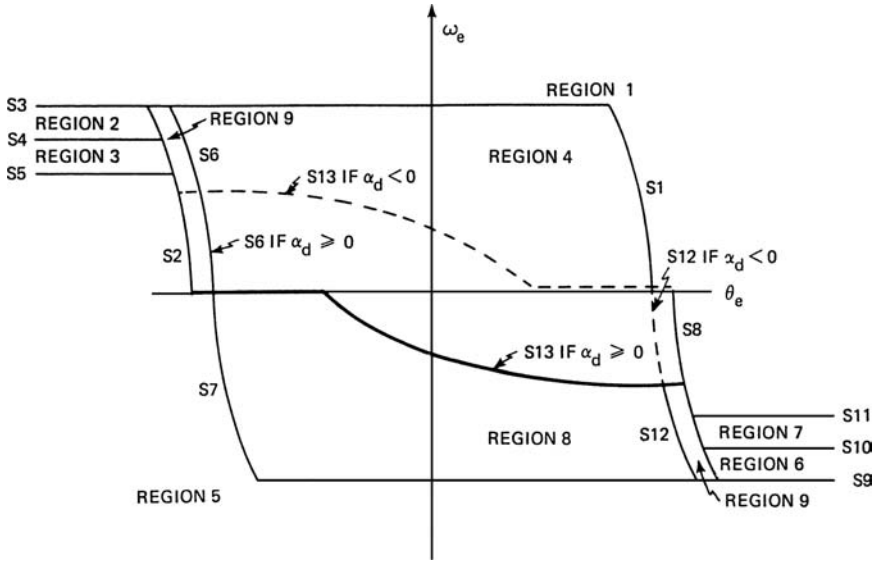

Fig. 7.9 Phase-plane logic for the Space Shuttle RCS.

Flight tests of this advanced autopilot system were successfully performed on STS missions 51G (June 1985) and 61B (November 1985).

7.6.2 Optimal Jet Selection Logic

The rotational equation of motion of a rigid spacecraft equipped with n jets can be approximated, neglecting the gyroscopic coupling terms, as

$$\mathbf{J}\dot{\boldsymbol{\omega}} = \mathbf{u} \Rightarrow \mathbf{J}\Delta\boldsymbol{\omega} = \sum_{j=1}^{n} \mathbf{a}_j \Delta t_j \tag{7.159}$$

where $\mathbf{J}$ is the inertia matrix of the spacecraft, $\boldsymbol{\omega} = (\omega_1, \omega_2, \omega_3)$ is the spacecraft angular velocity vector, $\Delta\boldsymbol{\omega} = (\Delta\omega_1, \Delta\omega_2, \Delta\omega_3)$, $\mathbf{u} = (u_1, u_2, u_3)$ is the control torque vector, and $\mathbf{a}_j$ is the torque vector of the jth jet with on-time Δt_j, all expressed in the spacecraft body-fixed control axes.

Equation (7.159) can be rewritten as

$$\mathbf{b} = \mathbf{A}\mathbf{x} \tag{7.160}$$

where $\mathbf{b} = \mathbf{J}\Delta\boldsymbol{\omega}$, $\mathbf{x} = (\Delta t_1, \ldots, \Delta t_n)$, and $\mathbf{A} = [a_{ij}] = [\mathbf{a}_1, \ldots, \mathbf{a}_n]$. That is, a_{ij} is the ith-axis torque caused by the j th jet firing with on-time x_j. It is assumed that $n > 3$ and rank$(\mathbf{A}) = 3$.

The translational equations of motion of a rigid spacecraft can be easily augmented to Eq. (7.160), resulting in an $m \times n$ torque/force distribution matrix $\mathbf{A}$ with $m \leq 6$ and rank $(\mathbf{A}) = m < n$. The optimal jet selection problem is then

to determine, in a fuel-optimal manner, a proper set of jets for the commanded angular/translational rate change in each axis. In general, a set of three jets are needed for the independent three-axis attitude control.

Consider an optimal jet selection logic concept that utilizes a linear programming approach for the minimum fuel problem formulated as

$$\min_{x_j} \sum_{j=1}^{n} c_j x_j = \mathbf{c}^T \mathbf{x} \tag{7.161}$$

where c_j is the jth jet flow rate, subject to the constraints

$$\mathbf{A}\mathbf{x} = \mathbf{b} \tag{7.162}$$

$$\mathbf{x} \geq 0 \tag{7.163}$$

Several important definitions and theorems often encountered in a linear programming problem with an $m \times n$ constant matrix $\mathbf{A}$ are summarized as follows [57].

Definition 7.4

1) A *feasible solution* to the linear programming problem is a vector $\mathbf{x} = (x_1, \ldots, x_n)$ that satisfies the constraints (7.162) and (7.163).

2) A *basis matrix* is an $m \times m$ nonsingular matrix formed from some m columns of the constraint matrix $\mathbf{A}$.

3) A *basic solution* to the linear programming problem is the unique vector $\mathbf{x}$ determined by choosing a basis matrix, letting the $n - m$ variables associated with columns of $\mathbf{A}$ not in the basis matrix equal zero.

4) A *basic feasible solution* is a basic solution in which all variables have nonnegative values.

5) A *nondegenerate basic feasible solution* is a basic feasible solution with exactly m positive x_j.

6) An *optimal solution* is a feasible solution that also minimizes the performance index (objective function) $J = \mathbf{c}^T \mathbf{x}$ in Eq. (7.161).

Theorem 7.4

The objective function $J = \mathbf{c}^T \mathbf{x}$ assumes its minimum at an extreme point of the constraint set (7.162) and (7.163). If it assumes its minimum at more than one extreme point, then it takes on the same value at every point of the line segment joining any two optimal extreme points.

Theorem 7.5

A vector $\mathbf{x}$ is an extreme point of the constraint set of a linear programming problem if and only if $\mathbf{x}$ is a basic feasible solution of the constraints (7.162) and (7.163).

These theorems imply that, in searching for an optimal solution, one needs only consider extreme points, i.e., only basic feasible solutions. An upper bound to the number of basic feasible solutions is given by

$$\frac{n!}{(n-m)!m!} = \frac{n(n-1)(n-2)\cdots(n-m+1)}{m!}$$

Consider an optimal jet selection problem of minimizing the objective function $J = \mathbf{c}^T\mathbf{x}$ with the constraint set (7.162) and (7.163). Although such an optimal jet selection problem has been studied previously in terms of an iterative linear programming approach [56,57], a new approach developed by Glandorf [58] and Kubiak and Johnson [59] appears to be more analytic and relatively concise. The algorithm developed in Refs. 58 and 59 is briefly described herein to introduce the reader to the essential feature of an optimal jet selection logic that can be executed recursively.

Let the constraint equation (7.162) be rewritten as

$$[\hat{\mathbf{A}} \quad \tilde{\mathbf{A}}] \begin{bmatrix} \hat{\mathbf{x}} \\ \tilde{\mathbf{x}} \end{bmatrix} = \mathbf{b} \tag{7.164}$$

and the objective function as

$$J = [\hat{\mathbf{c}}^T \quad \tilde{\mathbf{c}}^T] \begin{bmatrix} \hat{\mathbf{x}} \\ \tilde{\mathbf{x}} \end{bmatrix} = \hat{\mathbf{c}}^T\hat{\mathbf{x}} + \tilde{\mathbf{c}}^T\tilde{\mathbf{x}} \tag{7.165}$$

where $\hat{\mathbf{x}} \geq 0$, $\tilde{\mathbf{x}} = 0$, and $\hat{\mathbf{A}}$ is a nonsingular $m \times m$ matrix. Then a basic feasible solution is simply obtained as

$$\hat{\mathbf{x}} = \hat{\mathbf{A}}^{-1}\mathbf{b} \tag{7.166}$$

At this point, $\hat{\mathbf{A}}$ is not unique, and it represents a nonsingular $m \times m$ acceleration matrix corresponding to any combination of jets taken m at a time as long as they are linearly independent. To determine which of these combinations of jets are potentially optimal, one can assume there is a more efficient solution by allowing alternate jets to be turned on for a differential time, $\mathrm{d}\mathbf{x}$. That is, let

$$\hat{\mathbf{x}}' = \hat{\mathbf{x}} + \mathrm{d}\hat{\mathbf{x}}$$
$$\tilde{\mathbf{x}}' = \tilde{\mathbf{x}} + \mathrm{d}\tilde{\mathbf{x}} = \mathrm{d}\tilde{\mathbf{x}} \geq 0$$
$$J' = J + \mathrm{d}J$$

the constraint equation (7.162) then becomes

$$\hat{\mathbf{A}}\,\mathrm{d}\hat{\mathbf{x}} + \tilde{\mathbf{A}}\,\mathrm{d}\tilde{\mathbf{x}} = 0 \qquad \text{or} \qquad \mathrm{d}\hat{\mathbf{x}} = -\hat{\mathbf{A}}^{-1}\tilde{\mathbf{A}}\,\mathrm{d}\tilde{\mathbf{x}} \tag{7.167}$$

Using the objective function $J' = J + \mathrm{d}J$, one can obtain

$$\mathrm{d}J = \hat{\mathbf{c}}^T\,\mathrm{d}\hat{\mathbf{x}} + \tilde{\mathbf{c}}^T\,\mathrm{d}\tilde{\mathbf{x}} \tag{7.168}$$

Combining Eqs. (7.167) and (7.168), one can obtain the cost differential caused by $\mathrm{d}\tilde{\mathbf{x}}$ as

$$\begin{aligned}\mathrm{d}J &= \hat{\mathbf{c}}^T[-\hat{\mathbf{A}}^{-1}\tilde{\mathbf{A}}\,\mathrm{d}\tilde{\mathbf{x}}] + \tilde{\mathbf{c}}^T\,\mathrm{d}\tilde{\mathbf{x}} \\ &= [\tilde{\mathbf{c}}^T - \hat{\mathbf{c}}^T\hat{\mathbf{A}}^{-1}\tilde{\mathbf{A}}]\,\mathrm{d}\tilde{\mathbf{x}}\end{aligned} \tag{7.169}$$

Defining

$$\boldsymbol{\lambda}^T = \hat{\mathbf{c}}^T\hat{\mathbf{A}}^{-1}$$

where $\boldsymbol{\lambda}$ is called the optimality vector associated with $\hat{\mathbf{x}}$, and also defining $\tilde{\mathbf{a}}_i =$ the ith column of $\tilde{\mathbf{A}}$, i.e., $\tilde{\mathbf{a}}_i$ are the acceleration vectors for the jets not in the original selection, one can rewrite Eq. (7.169) as

$$\begin{aligned}\mathrm{d}J &= \tilde{\mathbf{c}}^T\,\mathrm{d}\tilde{\mathbf{x}} - \boldsymbol{\lambda}^T\tilde{\mathbf{A}}\,\mathrm{d}\tilde{\mathbf{x}} \\ &= \sum_{i=1}^{n-m}\tilde{c}_i\,\mathrm{d}\tilde{x}_i - \sum_{i=1}^{n-m}\boldsymbol{\lambda}^T\tilde{\mathbf{a}}_i\,\mathrm{d}\tilde{x}_i \\ &= \sum_{i=1}^{n-m}\left[\tilde{c}_i - \boldsymbol{\lambda}^T\tilde{\mathbf{a}}_i\right]\mathrm{d}\tilde{x}_i\end{aligned}$$

Assuming that all of the elements of $\mathbf{c}$ are unity without loss of generality, we obtain

$$\mathrm{d}J = \sum_{i=1}^{n-m}\left[1 - \boldsymbol{\lambda}^T\tilde{\mathbf{a}}_i\right]\mathrm{d}\tilde{x}_i \tag{7.170}$$

This equation is the key to determining whether the original selection of jets, i.e., $\hat{\mathbf{A}}$, is optimal or not. Therefore, if $\boldsymbol{\lambda}^T\tilde{\mathbf{a}}_i > 1$ for any jet not in the original selection, the original selection is not optimal and should be discarded. On the other hand, if $\boldsymbol{\lambda}^T\tilde{\mathbf{a}}_i \leq 1$ for all of the jets not in the original selection, then the original selection is potentially optimal and should be saved. These remaining k combinations or groups are referred to as candidate optimal groups (COGs) in Refs. 58 and 59.

The key properties of the optimality vector $\boldsymbol{\lambda}$ and COGs can be summarized as follows [59]:

1) For each COG, $\boldsymbol{\lambda}$ is perpendicular to the hyperplane in m-dimensional space formed by the end points of the m vectors $\{\hat{\mathbf{a}}_1, \ldots, \hat{\mathbf{a}}_m\}$ where $\hat{\mathbf{a}}_i$ is defined as the ith column of $\hat{\mathbf{A}}$.

2) The tips of the $\hat{\mathbf{a}}_i$ for a given COG define a surface segment of a hyperplane and all other surfaces or vertices for other COGs lie at or below this surface (closer to the origin than the surface).

3) The optimal COG is the COG with a maximum dot product of $\mathbf{b}$ and $\boldsymbol{\lambda}$.

4) After finding the optimal COGs, the jet on times are computed as $\hat{\mathbf{x}} = \hat{\mathbf{A}}^{-1}\mathbf{b}$ and $\tilde{\mathbf{x}} = 0$.

A more detailed description of the optimal jet select algorithm originally developed by Glandorf and Kubiak can be found in Refs. 58 and 59.

7.7 Pulse-Modulated Attitude Control

In the preceding section, the Space Shuttle on-orbit reaction control system was briefly described and the optimal jet selection problem of advanced space vehicles were introduced. The phase-plane logic described in the preceding section was used successfully for the Apollo and the Space Shuttle and may well continue as a basic architecture for future space vehicles. The phase-plane logic can have a great level of sophistication when implemented on a digital flight computer; however, it can be easily replaced by a simple Schmitt trigger for certain applications. In this section, conventional pulse modulation techniques, including the Schmitt trigger, as applied to the single-axis, on–off attitude control systems are described.

7.7.1 Introduction

Pulse modulation represents the common control logic behind most reaction-jet control systems of various spacecraft. Unlike other actuators, such as reaction wheels or control moment gyros, thruster output consists of two values: on or off. Proportional thrusters, whose fuel valves open a distance proportional to the commanded thrust level, are not employed much in practice. Mechanical considerations prohibit proportional valve operation largely because of dirt particles that prevent complete closure for small valve openings; fuel leakage through the valves consequently produces opposing thruster firings. Pulse modulation techniques have been developed that fully open and close the fuel valves, while producing a nearly linear duty cycle. In general, pulse modulators produce a pulse command sequence to the thruster valves by adjusting the pulse width and/or pulse frequency.

Several commonly used, flight-proven pulse modulators are briefly described in this section. Static characteristics are summarized for each modulator. The pulse frequency of these modulators are usually fast compared to the spacecraft attitude control bandwidth, and the static characteristics are often used for the modulator design. We consider here a simplified single-axis reaction control system for a rigid spacecraft as illustrated in Fig. 7.10.

7.7.2 Schmitt Trigger

Strictly speaking, this device, which is often called a relay with deadband/hysteresis, shown in Fig. 7.11, is not a pulse modulator. The advantage of this device, as opposed to other pulse modulators, is its simplicity. A disadvantage of the Schmitt trigger is the dependence of its static characteristics on the spacecraft inertia.

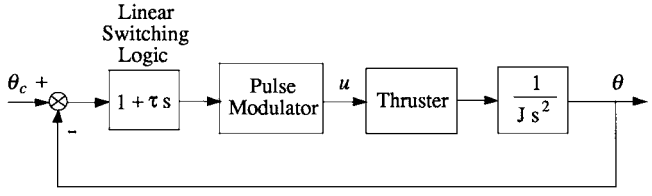

Fig. 7.10 Single-axis reaction control system.

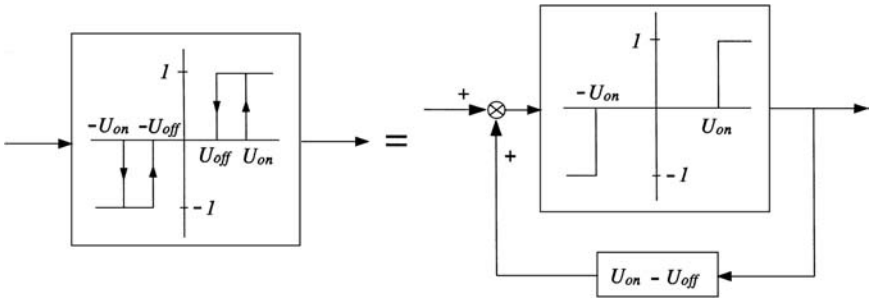

Fig. 7.11 Schmitt trigger.

If the pulse modulator in Fig. 7.10 is replaced by the Schmitt trigger, then the spacecraft dynamics can be described as

$$J\ddot{\theta} = T_c u \tag{7.171}$$

where

$$\begin{aligned} J &= \text{spacecraft inertia} \\ \theta &= \text{spacecraft attitude} \\ u &= \text{Schmitt trigger output } (0 \text{ or } \pm 1) \\ T_c &= \text{control torque level} \end{aligned}$$

and the input to the Schmitt trigger is determined by the linear switching logic $(1 + \tau s)(\theta_c - \theta)$.

The rigid-body limit cycling characteristics of this closed-loop system can be predicted, as follows:

$$\text{minimum pulse width} = \frac{Jh}{\tau T_c} \tag{7.172a}$$

$$\text{limit cycle amplitude} = \frac{T_c\,(U_{\text{on}} + U_{\text{off}})}{2} + \frac{J^2 h^2}{8\tau} \tag{7.172b}$$

$$\text{limit cycle period} = 4\tau \left(\frac{U_{\text{on}} + U_{\text{off}}}{h} + \frac{Jh}{2\tau^2} \right) \tag{7.172c}$$

where $h \equiv U_{\text{on}} - U_{\text{off}}$ and $\tau =$ the linear switching line slope.

Note that the minimum pulse width is a function of spacecraft parameters: the spacecraft inertia and thrust level. These parameters tend to change over time; as a result, the minimum pulse width will vary as well. Knowledge of the spacecraft properties is therefore required to estimate the thruster minimum pulse width.

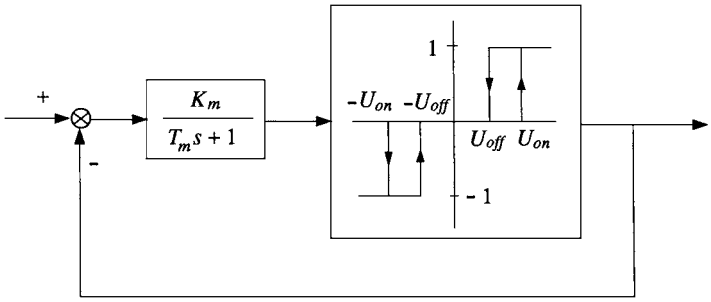

Fig. 7.12 PWPF modulator.

7.7.3 Pulse-Width Pulse-Frequency Modulator

The pulse-width pulse-frequency (PWPF) modulator has been used in the control systems of such spacecraft as the Agena satellite, INTELSAT V, INSAT, and ARABSAT. The device, as illustrated in Fig. 7.12, mainly comprises two components: a first-order lag filter and a Schmitt trigger inside a feedback loop. With a constant input, the PWPF modulator drives the thruster valve with an on–off pulse sequence having a nearly linear duty cycle with the input amplitude. The *duty cycle* or *modulation factor* is defined as the average output of the modulator.

The static characteristics of the PWPF modulator for a constant input E are summarized as follows for the thruster pulse width

$$T_{\text{on}} = -T_m \ln \left\{ \frac{(1-h)E_d - (E-1)}{E_d - (E-1)} \right\} \tag{7.173a}$$

the thruster off time

$$T_{\text{off}} = -T_m \ln \left\{ \frac{E_d - E}{(1-h)E_d - E} \right\} \tag{7.173b}$$

the pulse frequency

$$f = 1/(T_{\text{on}} + T_{\text{off}}) \tag{7.173c}$$

and the minimum pulse width

$$\Delta = -T_m \ln \left(1 - \frac{h}{K_m} \right) \approx \frac{hT_m}{K_m} \tag{7.173d}$$

where E = constant input magnitude, $E_d = U_{\text{on}}/K_m$ = equivalent internal deadband, and $h = U_{\text{on}} - U_{\text{off}}$. The duty cycle is given by $f\,T_{\text{on}}$ and it will be further discussed in Chapter 9.

In contrast to the Schmitt trigger, the static characteristics of the PWPF modulator are independent of the spacecraft inertia because of the feedback loop within the device. The presence of the filter and the feedback loop, however, inhibits linear analysis of the device's dynamic characteristics. The problem of designing a reaction jet control system employing the PWPF modulator will be further studied in Chapter 9.

7.7.4 Derived-Rate Modulator

The derived-rate and PWPF modulators are similar in format, as seen in Figs. 7.13 and 7.14, except that the first-order filter now compensates the Schmitt trigger output in the feedback path. The device is used much in the same way that the PWPF modulator is used, except that the derived-rate modulator introduces phase lead into a system as opposed to the PWPF modulator, which is a phase-lag device.

The static characteristics are similar to the PWPF modulator for the thruster pulse width

$$T_{\text{on}} = -T_m \, \ell n \left\{ 1 - \frac{h}{K_m - (E - U_{\text{on}})} \right\} \tag{7.174a}$$

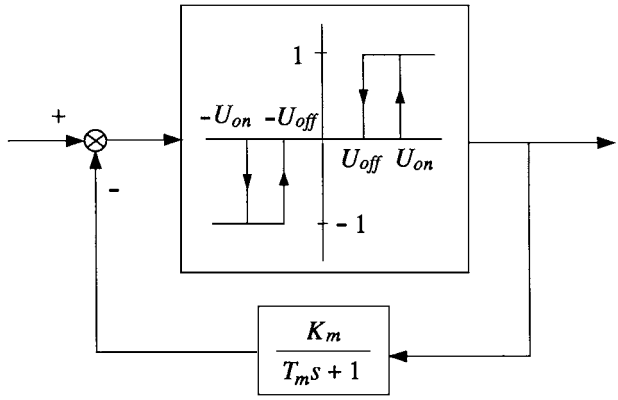

Fig. 7.13 Derived-rate modulator.

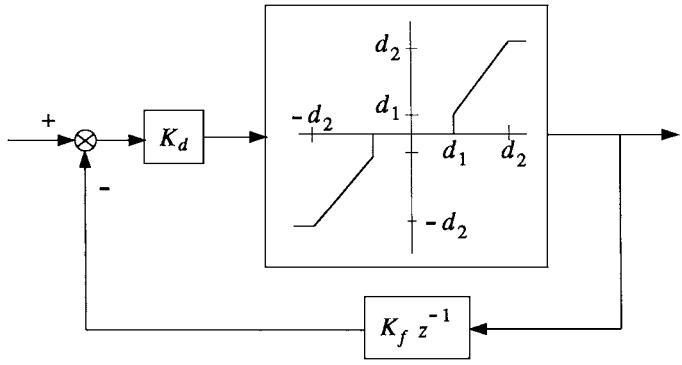

Fig. 7.14 Pulse-width modulator.

the thruster off time

$$T_{\text{off}} = T_m \, \ell n \left\{ 1 + \frac{h}{E - U_{\text{on}}} \right\} \tag{7.174b}$$

the pulse frequency

$$f = \frac{1}{T_{\text{on}} + T_{\text{off}}} \tag{7.174c}$$

and the minimum pulse width

$$\Delta \approx \frac{h \, T_m}{K_m} \tag{7.174d}$$

where E is the static input magnitude and the duty cycle is given by $f \, T_{\text{on}}$.

The derived-rate modulator is as difficult as the PWPF modulator to analyze in a limit cycling situation. In that case, the describing function method may be employed to characterize the modulator in terms of its gain and phase. This subject will be studied in detail in Chapter 9.

7.7.5 Pulse-Width Modulator

The pulse-width modulator (PWM) differs from the modulators discussed earlier in that it is essentially a discrete-time device; the PWPF and derived-rate modulators can be digitally implemented but are often analyzed as continuous-time systems.

The output of this particular device is not a thruster firing state as in the aforementioned devices; instead, the PWM output is thruster pulse width. A zero-order-hold (ZOH) device transmits that signal to the thrusters. The value d_1 represents the minimum pulse width of the system; this deadzone is directly proportional to the attitude deadband. The value d_2 represents the maximum pulse width of the RCS; it is equivalent to the microprocessor sampling period. As a result, the pulse frequency and the minimum pulse width of the modulator are fixed; a thruster firing command is given during every microprocessor sampling period even if the pulse is of zero width.

The delay in the feedback loop introduces damping to the system; maximum damping occurs when the feedback signal is smaller than the PWM input. If the input signal is not greater than the feedback signal, the modulator may limit the cycle itself. This criterion enables the designer to determine the feedback gain K_f. The feedforward gain K_d is selected as result of the minimum pulse criterion.

For more details of pulse modulation techniques as applied to spacecraft attitude control systems design, the reader is referred to Chapter 9, or Refs. 60–64.

References

[1] Rahn, C. D., and Barba, P. M., "Reorientation Maneuver for Spinning Spacecraft," *Journal of Guidance, Control, and Dynamics*, Vol. 14, No. 4, 1991, pp. 724–728.

[2] Bryson, A. E., Jr., *Control of Spacecraft and Aircraft*, Princeton Univ. Press, Princeton, NJ, 1994.

[3] Kaplan, M. H., *Modern Spacecraft Dynamics & Control*, Wiley, New York, 1976, pp. 367–379.

[4] Barba, P. M., and Aubrun, J. N., "Satellite Attitude Acquisition by Momentum Transfer," *AIAA Journal,* Vol. 14, No. 10, 1976, pp. 1382–1386.

[5] Scrivene, S. L., and Thompson, R. C., "Survey of Time-Optimal Attitude Maneuvers," *Journal of Guidance, Control, and Dynamics*, Vol. 17, No. 2, 1994, pp. 225–233.

[6] Bilimoria, K., and Wie, B., "Minimum-Time Large-Angle Reorientation of a Rigid Spacecraft," AIAA Paper 90-3486, Aug. 1990.

[7] Bilimoria, K., and Wie, B., "Time-Optimal Three-Axis Reorientation of a Rigid Spacecraft," *Journal of Guidance, Control, and Dynamics*, Vol. 16, No. 3, 1993, pp. 446–452.

[8] Bryson, A. E., Jr., and Ho, Y.-C., *Applied Optimal Control*, Hemisphere, Washington, DC, 1975.

[9] Athans, M., and Falb, P., *Optimal Control*, McGraw-Hill, New York, 1966.

[10] Li, F., and Bainum, P. M., "Numerical Approach for Solving Rigid Spacecraft Minimum Time Attitude Maneuvers," *Journal of Guidance, Control, and Dynamics*, Vol. 13, No. 1, 1990, pp. 38–45.

[11] Bilimoria, K., and Wie, B., "Time-Optimal Reorientation of a Rigid Axisymmetric Spacecraft," *Proceedings of the AIAA Guidance, Navigation, and Control Conference*, AIAA, Washington, DC, 1991, pp. 422–431.

[12] Byers, R. M., and Vadali, S. R., "Quasi-Closed-Form Solution to the Time-Optimal Rigid Spacecraft Reorientation Problem," *Journal of Guidance, Control, and Dynamics*, Vol. 16, No. 3, 1993, pp. 453–461.

[13] Seywald, H., and Kumar, R. R., "Singular Control in Minimum Time Spacecraft Reorientation," *Journal of Guidance, Control, and Dynamics*, Vol. 16, No. 4, 1993, pp. 686–694.

[14] Bauer, F. H., Femiano, M. D., and Mosier, G. E., "Attitude Control System Conceptual Design for the X-ray Timing Explorer," *Proceedings of the AIAA Guidance, Navigation, and Control Conference*, AIAA, Washington, DC, 1992, pp. 236–249.

[15] Wie, B., and Barba, P. M., "Quaternion Feedback for Spacecraft Large Angle Maneuvers," *Journal of Guidance, Control, and Dynamics*, Vol. 8, No. 3, 1985, pp. 360–365.

[16] Wie, B., Weiss, H., and Arapostathis, A., "Quaternion Feedback Regulator for Spacecraft Eigenaxis Rotations," *Journal of Guidance, Control, and Dynamics*, Vol. 12, No. 3, 1989, pp. 375–380.

[17] Wie, B. and Lu, J., "Feedback Control Logic for Spacecraft Eigenaxis Rotations Under Slew Rate and Control Constraints," *Journal of Guidance, Control, and Dynamics*, Vol. 18, No. 6, 1995, pp. 1372–1379.

[18] Wie, B., Byun, K.-W., Warren, W., Geller, D., Long, D., and Sunkel, J., "New Approach to Momentum/Attitude Control for the Space Station," *Journal of Guidance, Control, and Dynamics*, Vol. 12, No. 5, 1989, pp. 714–722.

[19] Wie, B., Liu, Q., and Sunkel, J., "Robust Stabilization of the Space Station in the Presence of Inertia Matrix Uncertainty," *Journal of Guidance, Control, and Dynamics*, Vol. 18, No. 3, 1995, pp. 611–617.

[20] Byun, K.-W., Wie, B., Geller, D., and Sunkel, J., "Robust H_∞ Control Design for the Space Station with Structured Parameter Uncertainty," *Journal of Guidance, Control, and Dynamics*, Vol. 14, No. 6, 1991, pp. 1115–1122.

[21] Rhee, I., and Speyer, J. L., "Robust Momentum Management and Attitude Control System for the Space Station," *Journal of Guidance, Control, and Dynamics*, Vol. 15, No. 2, 1992, pp. 342–351.

[22] Balas, G. J., Packard, A. K., and Harduvel, J. T., "Application of μ-Synthesis Technique to Momentum Management and Attitude Control of the Space Station," *Proceedings of the AIAA Guidance, Navigation, and Control Conference*, AIAA, Washington, DC, 1991, pp. 565–575.

[23] Jacot, A. D., and Liska, D. J., "Control Moment Gyros in Attitude Control," *Journal of Spacecraft and Rockets*, Vol. 3, No. 9, 1966, pp. 1313–1320.

[24] Chubb, W. B., and Epstein, M., "Application of Control Moment Gyros to the Attitude Control of the Apollo Telescope Unit," *Proceedings of AIAA Guidance, Control, and Flight Mechanics Conference*, AIAA, New York, 1968.

[25] Kennel, H. F., "A Control Law for Double-Gimballed Control Moment Gyros Used for Space Vehicle Attitude Control," NASA TM-64536, Aug. 1970.

[26] Austin, F., Liden, S., and Berman, H., "Study of Control Moment Gyroscope Applications to Space Base Wobble Damping and Attitude Control Systems," Grumman Aerospace Corp., CR NAS 9-10427, National Technical Information Service, N71-11401, Springfield, VA, Sept. 1970.

[27] Ranzenhofer, H. D., "Spacecraft Attitude Control with Control Moment Gyros," *Proceedings of AIAA Guidance, Control, and Flight Mechanics Conference*, AIAA, New York, 1971.

[28] Powell, B. K., Lang, G. E., Lieberman, S. I., and Rybak, S. C., "Synthesis of Double Gimbal Control Moment Gyro Systems for Spacecraft Attitude Control," *Proceedings of AIAA Guidance, Control, and Flight Mechanics Conference*, AIAA, New York, 1971.

[29] Ross, C. H., and Worley, E., "Optimized Momentum and Attitude Control System for Skylab," *Proceedings of AIAA Guidance, Control, and Flight Mechanics Conference*, AIAA, New York, 1971.

[30] Yoshikawa, T., "A Steering Law for Three Double-Gimballed Control Moment Gyro System," NASA TMX-64926, March 1975.

[31] Yoshikawa, T., "Steering Law for Roof-Type Configuration Control Moment Gyro System," *Automatica*, Vol. 13, No. 4, 1977, pp. 359–368.

[32] Margulies, G., and Aubrun, J.-N., "Geometric Theory of Single-Gimbal Control Moment Gyro Systems," *Journal of the Astronautical Sciences,* Vol. 26, No. 2, 1978, pp. 159–191.

[33] Cornick, D. E., "Singularity Avoidance Control Laws for Single Gimbal Control Moment Gyros," *Proceedings of the AIAA Guidance and Control Conference*, AIAA, New York, 1979, pp. 20–33.

[34] Kennel, H. F., "Steering Law for Parallel Mounted Double-Gimballed Control Moment Gyros—Revision A," NASA TM-82390, Jan. 1981.

[35] Kennel, H. F., "Double-Gimballed Control Moment Gyro Steering Law Update," NASA Internal Memo ED12-86-52, May, 1986.

[36] Kurokawa, H., Yajima, S., and Usui, S., "A New Steering Law of a Single-Gimbal CMG System of Pyramid Configuration," *Proceedings of the 10th IFAC Symposium on Automatic Control in Space*, Pergamon, Oxford, England, UK, 1985, pp. 249–255.

[37] Paradiso, J. A., "A Highly Adaptable Steering/Selection Procedure for Combined CMG/RCS Spacecraft Control," *Advances in Astronautical Sciences*, Vol. 61, Feb. 1986, pp. 263–280.

[38] Branets, V. N., et al., "Development Experience of the Attitude Control System Using Single-Axis Control Moment Gyros for Long-Term Orbiting Space Stations," *38th Congress of the International Astronautical Federation*, IAF-87-04, Oct. 1987.

[39] Bedrossian, N. S., Paradiso, J., Bergmann, E. V., and Rowell, D., "Steering Law Design for Redundant Single-Gimbal Control Moment Gyroscopes," *Journal of Guidance, Control, and Dynamics*, Vol. 13, No. 6, 1990, pp. 1083–1089.

[40] Bedrossian, N. S., Paradiso, J., Bergmann, E. V., and Rowell, D., "Redundant Single-Gimbal Control Moment Gyroscope Singularity Analysis," *Journal of Guidance, Control, and Dynamics*, Vol. 13, No. 6, 1990, pp. 1096–1101.

[41] Vadali, S. R., Oh, H., and Walker, S., "Preferred Gimbal Angles for Single Gimbal Control Moment Gyroscopes," *Journal of Guidance, Control, and Dynamics*, Vol. 13, No. 6, 1990, pp. 1090–1095.

[42] Dzielski, J., Bergmann, E., Paradiso, J. A., Rowell, D., and Wormley, D., "Approach to Control Moment Gyroscope Steering Using Feedback Linearization," *Journal of Guidance, Control, and Dynamics*, Vol. 14, No. 1, 1991, pp. 96–106.

[43] Oh, H.-S., and Vadali, S. R., "Feedback Control and Steering Laws for Spacecraft Using Single Gimbal Control Moment Gyroscopes," *Journal of the Astronautical Sciences*, Vol. 39, No. 2, 1991, pp. 183–203.

[44] Paradiso, J. A., "Global Steering of Single Gimballed Control Moment Gyroscopes Using a Direct Search," *Journal of Guidance, Control, and Dynamics*, Vol. 15, No. 5, 1992, pp. 1236–1244.

[45] Hoelscher, B. R., and Vadali, S. R., "Optimal Open-Loop and Feedback Control Using Single Gimbal Control Moment Gyroscopes," *Journal of the Astronautical Sciences*, Vol. 42, No. 2, 1994, pp. 189–206.

[46] Kurokawa, H., "Exact Singularity Avoidance Control of the Pyramid Type CMG System," *Proceedings of the AIAA Guidance, Navigation, and Control Conference*, AIAA, Washington, DC, 1994, pp. 170–180.

[47] Vadali, S. R., and Krishnan, S., "Suboptimal Command Generation for Control Moment Gyroscopes and Feedback Control of Spacecraft," *Journal of Guidance, Control, and Dynamics*, Vol. 18, No. 6, 1995, pp. 1350–1354.

[48] "Technical Description Document for the PG-1 Guidance, Navigation and Control System," Space Station Div., MDC 95H0223, McDonnell Douglas Aerospace, Houston, TX, March 1996.

[49] Kurokawa, H., "Constrained Steering Law of Pyramid-Type Control Moment Gyros and Ground Tests," *Journal of Guidance, Control, and Dynamics*, Vol. 20, No. 3, 1997, pp. 445–449.

[50] Heiberg, C. J., Bailey, D., and Wie, B., "Precision Pointing Control of Agile Spacecraft Using Single-Gimbal Control Moment Gyros," *Journal of Guidance, Control, and Dynamics*, Vol. 23, No. 1, 2000, pp. 77–85.

[51] Meffe, M., and Stocking, G., "Momentum Envelope Topology of Single-Gimbal CMG Arrays for Space Vehicle Control," AAS Paper No. 87-002, Jan. 31–Feb. 4, 1987.

[52] Nakamura, Y., and Hanafusa, H., "Inverse Kinematic Solutions with Singularity Robustness for Robot Manipulator Control," *Journal of Dynamic Systems, Measurement and Control*, Vol. 108, Sept. 1986, pp. 163–171.

[53] "Shuttle On-Orbit Flight Control Characterization (Simplified Digital Autopilot Model)," C. S. Draper Lab., NASA, JSC 18511, Aug. 1982.

[54] Hattis, P. D., "Qualitative Differences Between Shuttle On-Orbit and Transition Control," *Journal of Guidance, Control, and Dynamics*, Vol. 7, No. 1, 1984, pp. 4–8.

[55] Cox, K. J., and Hattis, P. D., "Shuttle Orbit Flight Control Design Lessons: Direction for Space Station," *Proceedings of the IEEE*, Vol. 75, No. 3, 1987, pp. 336–355.

[56] Bergmann, E. V., Croopnick, S. R., Turkovich, J. J., and Works, C. C., "An Advanced Spacecraft Autopilot Concept," *Journal of Guidance and Control*, Vol. 2, No. 3, 1979, pp. 161–168.

[57] Luenberger, D. G., *Linear and Non-linear Programming*, 2nd ed., Addison–Wesley, Reading, MA, 1989.

[58] Glandorf, D. R., "An Innovative Approach to the Solution of a Class of Linear Programming Problems," Lockheed Engineering and Management Services Co., Inc., LEMSCO-23244, Houston, TX, Nov. 1986.

[59] Kubiak, E. T., and Johnson, D. A., "Optimized Jet Selection Logic," NASA Internal Memo EH2-87L-038, March 1987.

[60] Wie, B., and Plescia, C. T., "Attitude Stabilization of a Flexible Spacecraft During Stationkeeping Maneuvers," *Journal of Guidance, Control, and Dynamics*, Vol. 7, No. 4, 1984, pp. 430–436.

[61] Anthony, T., Wie, B., and Carroll, S., "Pulse-Modulated Controller Synthesis for a Flexible Spacecraft," *Journal of Guidance, Control, and Dynamics*, Vol. 13, No. 6, 1990, pp. 1014–1022.

[62] Song, G., Buck, N., and Agrawal, B., "Spacecraft Vibration Reduction Using Pulse-Width Pulse-Frequency Modulated Input Shaper," *Proceedings of the 1997 AIAA Guidance, Navigation, and Control Conference*, AIAA, Reston, VA, 1997, pp. 1535–1549.

[63] Ieko, T., Ochi, Y., and Kanai, K., "A New Digital Redesign Method for Pulse-Width Modulation Control Systems," *Proceedings of the 1997 AIAA Guidance, Navigation, and Control Conference*, AIAA, Reston, VA, 1997, pp. 1730–1737.

[64] Bernelli-Zazzera, F., Mantegazza, P., and Nurzia, V., "Multi-Pulse-Width Modulated Control of Linear Systems," *Journal of Guidance, Control, and Dynamics*, Vol. 21, No. 1, 1998, pp. 64–70.